Using Machine Learning Models to Analyze the Aerodynamic Properties of Airfoils

Aaron Wong and Ronil Synghal

6/20/22 *(date completed)*
<course if you want, other information that's relevant>

Abstract

In aerodynamics, the lift-drag ratio of an airfoil is of paramount importance, as it directly correlates with fuel efficiency. Traditionally, determining airfoil properties necessitates expensive experimental tests or computationally intensive simulations. This research posits that leveraging artificial intelligence could significantly reduce financial and computational costs while identifying optimal airfoil geometries. The data originates from Bigfoil, a database of airfoils compiled from UIUC's database, Javafoil, and NACA tested airfoils. Specifically, we employed a convolutional neural network (CNN) to analyze various airfoil images and geometric data. The image data provides the machine learning system a visual understanding of the airfoil, and allows it to pinpoint aerodynamic properties to different shapes. Our model, constructed with multiple Conv2D layers and auxiliary components, was designed to predict the lift-to-drag ratio. Preliminary results were promising: the optimal CNN configuration accurately predicted the ratios for 58.6% of previously unseen airfoils. However, there remains potential for improvement. Enhanced hyperparameter tuning could further augment the prediction accuracy. Additionally, utilizing higher-resolution images and improving image quality enhance the network's predictive capabilities.

Introduction and Background

Aerodynamics pertains to studying airflow behavior when interacting with solid bodies. A critical component of this domain is the design of airfoils, which significantly influence airplane performance. There are four primary forces exerted on an aircraft during flight [1]. Firstly, the thrust is the propulsive force typically generated by the engine, acting in the direction the engine propels. Secondly, the gravitational force resulting from the airplane's mass leads to a downward force termed weight.

The third and fourth forces, lift and drag, originate predominantly from the aircraft's wings. Lift is produced per Bernoulli's principle. The lift force always acts perpendicular to the relative wind direction[2]. Conversely, drag arises due to various factors, including vortices, air resistance against the wing's leading edge, flow separation, and skin friction. While drag stemming from flow separation and vortices, termed induced drag, acts parallel to the relative wind direction, other forms of drag resist the aircraft's forward motion[3].

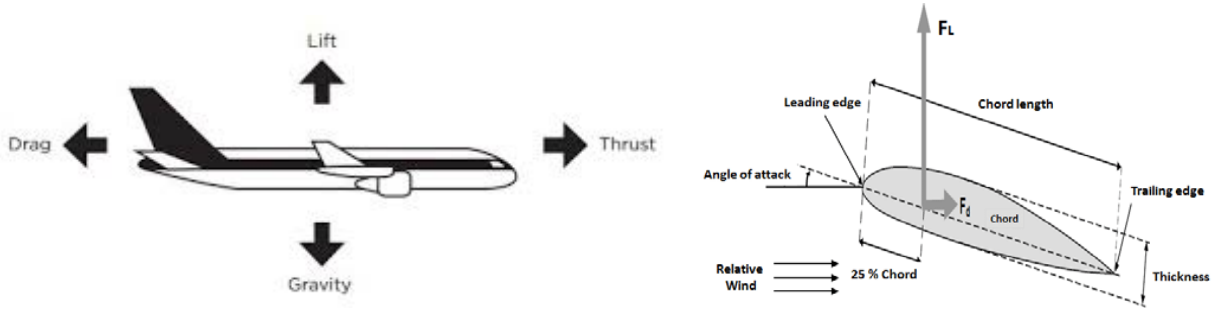

Figure 1a and 1b : The four forces of an airplane in their general directions[1]. Aerodynamic Forces generated by an Airfoil. As displayed, lift always acts perpendicular to the relative wind and drag always acts parallel to the relative wind despite having an angle of attack.

Though supersonic drag is another form of resistance, it is beyond the scope of this paper. The mathematical representations for lift and drag are defined with the following parameters: C_d represents the Coefficient of Drag for an airfoil, C_l symbolizes the Coefficient of Lift, ρ (rho) stands for air density, v signifies the flow velocity around the aircraft, and S denotes the wing's surface area[4].

$$F_{drag} = C_d * \rho * S * v^2 \qquad F_{lift} = C_l * \rho * S * v^2$$

An airfoil refers to the cross-sectional profile of an airplane wing, taken perpendicular to the wing's span. The specific geometry of an airfoil fundamentally dictates its associated lift and drag coefficients. The following section elucidates the principal geometric descriptors of an airfoil[5].

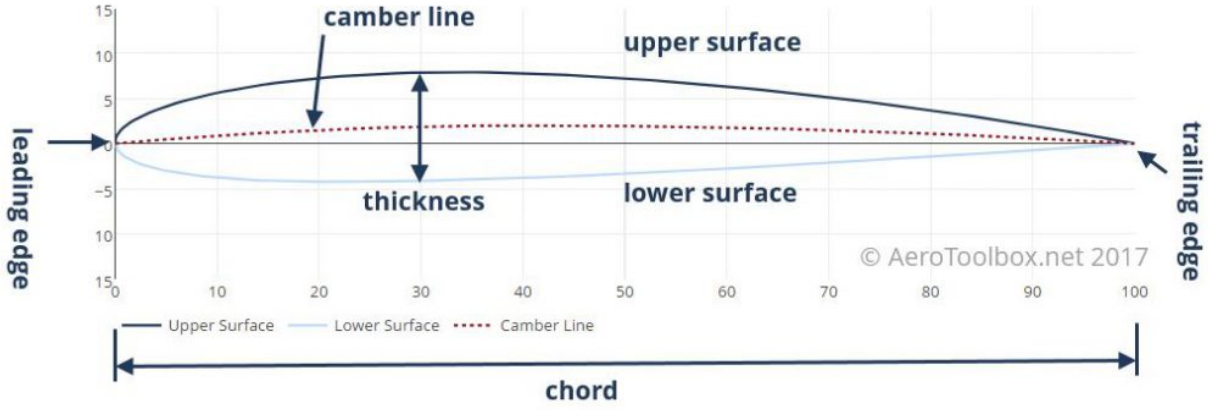

Figure 2: Main features of an airfoil

- Mean Camber Line: Representing the locus of midpoints between the upper and lower surfaces of an airfoil, the mean camber line is derived by averaging the y-values corresponding to the same x-value on both surfaces.
- Leading & Trailing Edge: The foremost and the rearmost boundaries of an airfoil are termed its leading and trailing edges, respectively.
- Chord Line: A linear segment directly linking the leading and trailing edges of the airfoil.
- Camber: Defined as the greatest perpendicular distance between the mean camber line and the chord line. To facilitate lift, it is generally favored for the mean camber line to situate above the chord line.
- Thickness: Representing the airfoil's profile robustness, it is the maximum separation between its upper and lower surfaces.[6]
- Angle of Attack (α): Quantified as the angle formed between the oncoming relative wind and the chord line. Notably, different angles of attack correspond to varied lift and drag coefficients. Within the context of our dataset, it's assumed that aircraft predominantly cruise at an angle optimizing efficiency,[7]

- Reynold's Number: A dimensionless parameter pivotal for predicting fluid dynamics, it's given by the formula: $Re=\frac{\rho v l}{\mu}$. Where: ρ is the air density, v is the fluid velocity, l is the airfoil's chord length, μ is the fluid's dynamic viscosity.
- Mach Number: A ratio comparing an object's speed to the speed of sound. Conventionally, Mach 1 corresponds to approximately 343 m/s, thus, Mach 2 equates to roughly 686 m/s.[8]

The lift-to-drag coefficient ratio holds profound importance in aerodynamics, reflecting directly upon the corresponding force ratios. For aircraft of smaller dimensions, an elevated lift/drag ratio signifies the capability to sustain flight at reduced speeds. This corresponds to diminished drag, translating to a lesser thrust requirement to maintain a cruising velocity. In contrast, a superior ratio indicates reduced drag for larger aircraft, thus yielding enhanced efficiency and minimized fuel expenditures. Even a 1% increase in lift-drag ratio can significantly increase the payload of the aircraft by 2800 lbs for a given range[9].

Traditionally, ascertaining airfoil properties hinges on methodologies like wind tunnel testing or computer-aided simulations. However, both avenues come with constraints. Wind tunnel setups necessitate extensive capital for establishment and sustenance, while computer simulations demand formidable computational prowess[10]. Across 23 different wind tunnels analyzed at NASA, the average cost to maintain a wind tunnel annually was around 2.2 million dollars, with some maintenance costs reaching over 11 million dollars. The average replacement value (or the cost of each individual wind tunnel) of each of these wind tunnels is 127 million [11].

Machine learning emerges as a promising alternative, with the potential to approximate the lift-to-drag ratio of airfoils without substantial costs or computational overhead. This technique could equip aerospace engineers with invaluable insights into the nuances of optimal airfoil geometry. Supporting this assertion, Song et al. noted in their abstract, "Compared with the traditional genetic algorithm method, the machine learning-based approach showcases superior aerodynamic performance coupled with significantly reduced simulation durations for identical airfoil optimization challenges. Prospective applications of machine learning methods exhibit immense promise in fluid machinery design optimization [12]." This highlights the burgeoning potential of AI-driven methodologies to revolutionize airfoil design optimization.

In this work, our attention is directed towards the dataset of airfoils available on Bigfoil.com. By integrating both the visual data of airfoil profiles (refer to Figure 1) and the numerical data from the Big Table (refer to Figure 2) specific to a Reynolds Number of 3 million, our objective is to construct a predictive model capable of determining the lift-to-drag ratio for various airfoil configurations.

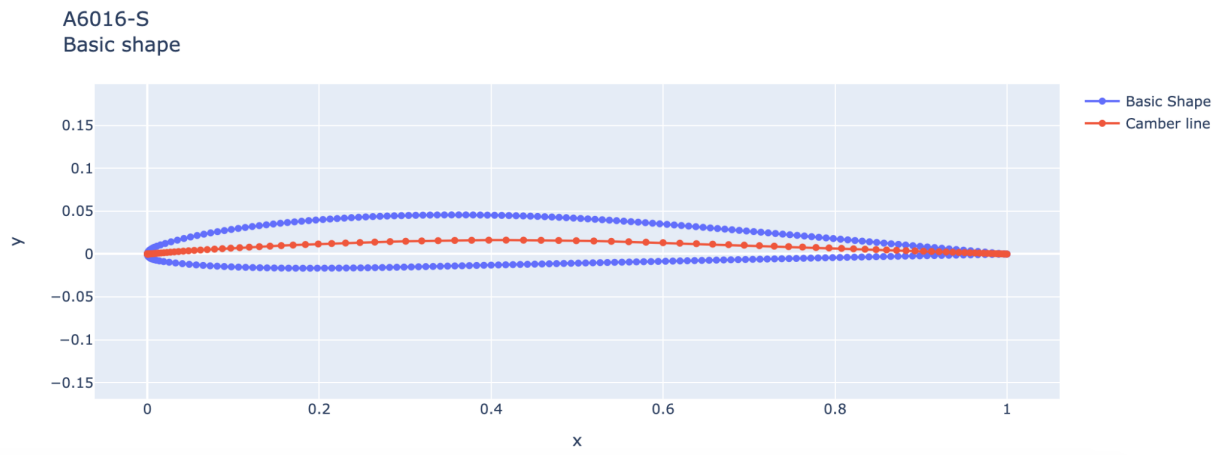

Figure 3: Each wing has an image associated containing the basic shape and the camber line

Metadata		Geometry			Data (JavaFoil at Re=3M, Mach 0, smooth)	
Name ↓↑	Family ↓↑	↓↑Thickness (%)	↓↑x-Location of Max Thk (%)	↓↑Camber (%)	↓↑Cl Max	↓↑Cl/Cd Max
63A108 MOD C	NASA	7.7	30.1	0.6	1.02	64
A18	Uncategorized	7.3	30.1	3.2	1.40	84
A18 (SMOOTHED)	Uncategorized	7.3	26.5	3.8	1.31	85
A6014-S	Ayers	6.0	30.1	1.4	0.70	88
A6016-S	Ayers	6.0	30.1	1.6	0.77	89
A6018-S	Ayers	6.0	31.9	1.8	0.77	96
A6020-S	Ayers	6.0	31.9	2.0	0.80	98
A6516-S	Ayers	6.5	30.1	1.6	0.70	89
A6518-S	Ayers	6.5	31.9	1.8	0.82	105
A6520-S	Ayers	6.6	31.9	2.0	0.85	107
A6522-S	Ayers	6.5	31.9	2.1	0.86	111
A7018-S	Ayers	7.0	30.1	1.8	0.87	102
A7020-S	Ayers	7.0	31.9	1.9	0.92	104
A7022-S	Ayers	7.0	31.9	2.2	0.88	110
A7024-S	Ayers	7.0	31.9	2.4	0.93	119

Figure 4: The big table contains Name, Family, Thickness, x-thickness data, camber line data, max lift coefficient, and lift/drag max. The lift and lift/drag varies. The table values display the max values at the optimal angle of attack.

Past Works

Machine learning, particularly the application of Convolutional Neural Networks (CNNs), has progressively found its footing in the study of fluid mechanics in recent years. Several critical contributions to this domain are noteworthy. Bhatnagar et al. [13] successfully used CNNs to predict velocity and pressure fields, showcasing the versatility of the approach. Sekar et al. employed CNNs to approximate the flow field over an airfoil. Their model integrated multiple parameters, including Reynolds Number, airfoil geometry, and angle of attack [14]. Hui et al. utilized CNNs to predict pressure distribution encompassing airfoils [15]. This modeling was typically done by force transducers. Guo et al. broadened the application spectrum of CNNs by studying and forecasting non-uniform steady laminar flow within 2-D and 3-D domains. Their methodology notably achieved estimations at a rate two orders of magnitude faster than conventional GPU-based CFD solvers [16].

Related Works

Several studies have embarked on the journey of harnessing machine learning and computational tools to predict aerodynamic properties:

Zhang et al.: Most analogous to our study, Zhang and his team utilized visual imagery to predict lift coefficients under specific parameters: angle of attack, Reynolds Numbers, and Mach Numbers. Their findings indicate that a CNN does a regional job in predicting the lift coefficient at a certain angle of attack [17].

Moin et al.: This research focused on NACA 4-digit and 5-digit airfoils. Leveraging the Javafoil software, they generated a sequence of over 101 spaced points, to create smooth upper and lower edges [18]. Furthermore, Javafoil was employed to compute specific coefficients: Lift, Drag, and Moment (the latter is an airfoil coefficient indicating stability rather than fuel efficiency). These calculations were made with respect to various Mach numbers, Reynolds Numbers, and angles of attack. Their results underline the efficacy of Artificial Neural Networks (ANNs) in predicting aerodynamic attributes solely based on the airfoil coordinates.
Takaki et al. identified a strong correlation between the Reynolds number within the flow field and the L/D ratio inherent to an airfoil [19].

Our research endeavors to synthesize elements from Zhang et al., Moin et al., and Takaki et al. We aim to incorporate both visual imagery and pivotal geometric metrics associated with an airfoil to predict the maximum lift-to-drag ratios.

2. Dataset

Dataset Introduction

The dataset employed in this study was procured from BigFoil which compiled UIUC Airfoil Coordinates Database or generated programmatically by Martin Hepperle's JavaFoil. A handful of sections were sourced from NACA-TR-824 and other freely available sources, all put together on Bigfoil, Utilizing a Python-based scraping approach facilitated by the Beautiful Soup package, the data was scraped and formatted… . Bigfoil.com stands as a comprehensive repository encompassing over 6,000 airfoils sourced from an array of airfoil design companies and manufacturers. Out of the 6,316 airfoils harvested, a subset of 6,147 was deemed appropriate for analysis, possessing the requisite data compatible with the neural network's evaluation criteria. Each airfoil within this subset is characterized by visual representations (refer to Figure #) as well as raw numerical data delineating its geometric attributes (refer to Figure 5).

Preprocessing

Metadata				Geometry			Data (JavaFoil at Re=3M, Mach 0, smooth)				
Name ↓↑	Link	Family ↓↑	Data Sources	↓↑Thicknes...	↓↑x-Locatio...	↓↑Camber (...	↓↑Cl Max	↓↑Cl/Cd Max	↓↑Cd @ Cl=...	↓↑Cd @ Cl=...	↓↑Cd @ Cl=...
63A108 MOD C	63A108 MOD C	NASA	JF XF	7.7	30.1	0.6	1.02	64	0.011	0.013	0.013
A18	A18	Uncategorized	JF WT XF	7.3	30.1	3.2	1.40	84	0.011	0.011	0.01
A18 (SMOOTHE...	A18 (smoothed)	Uncategorized	JF XF	7.3	26.5	3.8	1.31	85	0.011	0.011	0.01
A6014-S	A6014-S	Ayers	JF XF	6.0	30.1	1.4	0.70	88	0.005	0.005	0.067
A6016-S	A6016-S	Ayers	JF XF	6.0	30.1	1.6	0.77	89	0.005	0.006	0.072
A6018-S	A6018-S	Ayers	JF XF	6.0	31.9	1.8	0.77	96	0.005	0.004	0.072
A6020-S	A6020-S	Ayers	JF XF	6.0	31.9	2.0	0.80	98	0.007	0.004	0.072
A6516-S	A6516-S	Ayers	JF XF	6.5	30.1	1.6	0.70	89	0.005	0.005	0.063
A6518-S	A6518-S	Ayers	JF XF	6.5	31.9	1.8	0.82	105	0.006	0.004	0.075
A6520-S	A6520-S	Ayers	JF XF	6.6	31.9	2.0	0.85	107	0.006	0.004	0.080
A6522-S	A6522-S	Ayers	JF XF	6.5	31.9	2.1	0.86	111	0.007	0.004	0.080
A7018-S	A7018-S	Ayers	JF XF	7.0	30.1	1.8	0.87	102	0.006	0.004	0.079
A7020-S	A7020-S	Ayers	JF XF	7.0	31.9	1.9	0.92	104	0.006	0.004	0.086
A7022-S	A7022-S	Ayers	JF XF	7.0	31.9	2.2	0.88	110	0.007	0.004	0.077
A7024-S	A7024-S	Ayers	JF XF	7.0	31.9	2.4	0.93	119	0.007	0.004	0.084

Figure 5: All of the columns of Bigtable

The initial steps of preprocessing included the exclusion of hyperlinks leading to individual airfoils and eliminating superfluous attributes like CdCl01, CdCl04, and CdCl06. To address data gaps, especially within geometric metrics such as thickness, x-thickness, and camber, we deployed imputation techniques, replacing missing values with the respective overall mean values of all other data values for each parameter.

Additionally, the 'family' attribute, which denotes airfoil classifications, underwent a transformation using a label encoder. Although, at first glance, the 'family' attribute might not directly pertain to an airfoil's performance, it potentially holds implicit insights. As demonstrated in Figure 3, a discernible variance in airfoil performance relative to the LD Max can be attributed to distinct 'families' or manufacturers. Due to their design philosophies or technological prowess, some manufacturers might craft superior airfoils, and thus this attribute was retained as a variable of consideration in our analysis.

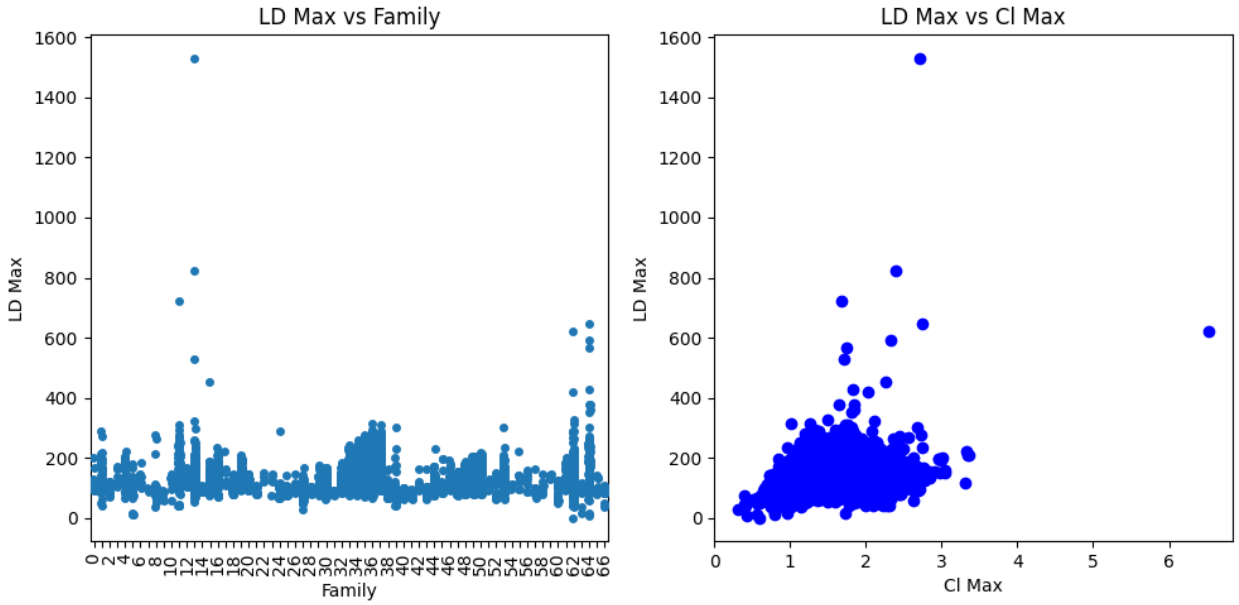

Figures 6A show the LD Max distribution by different companies. Each family has been encoded with a numerical value. **Figure 6B** show a generally positive relationship between C_l Max and LD Max, making it a good input.

The visual data of the airfoils also underwent significant preprocessing. We reduced the image size via interpolation to speed up the neural network and due to the limitations of computational resources. Using the T4 GPU on Google Collaboratory provided some limits on available resources and so the reduction of image size helped ensure our code ran in a timely manner.

A structured approach was adopted to pair each image with its respective Lift-to-Drag (LD) Max value. Leveraging the unique naming convention of each image file, which corresponded to the airfoil name, we established a dictionary with key-value pairs representing "Name" and "LD Max." A parallel procedure was implemented to match the geometric data, and the family attributes with the associated image data.

The dataset was then partitioned with 75% of our data allocated for training while 25% of our data allocated for testing.

Data significance

Incorporating image data plays a pivotal role in enhancing the AI model's ability to interpret the airfoil's geometry and design nuances which affect its lift to drag properties. On the other hand, the geometric data provides raw, quantitative information about the airfoil. Such data could improve the accuracy of the model's predictions as compared to just picture data. As illustrated in Figure 3B, there is a discernible positive correlation between LD Max and Cl Max. This trend, along with other relationships observed in the geometric data, underscores the importance of these attributes and their bearing on the LD Max.

To channel the scope of this research toward understanding the efficiency dynamics of airplanes rather than a broad prediction of airfoil attributes, specific parameters like the angle of attack and Reynolds Numbers have been deliberately excluded from the model's input variables. For the purposes of this research, the angle of attack is assumed to be angled such that the Lift/Drag properties is at its max.

3. Methodology / Models

Convolutional Neural Network

We used a Convolutional Neural Network (CNN) for our analytical framework, constructed using the Keras library. Given that the data comprises both image and numerical attributes— the architecture must process both data types individually before combining models and nodes to generate an output. The overall structure of the model sees an overall artificial neural network with two networks, convolutional and neural, to process the respective image and numerical data.

The image data is processed through the CNN in a sequential manner. Initially, the image undergoes several Conv2D layers, where convolution operations are performed using designated kernels [20]. These kernels essentially slide over the image, extracting pivotal features. Subsequent to the convolution operation, Max Pooling is executed. This process condenses the kernel-processed data by selecting the maximum value from a defined portion of the kernel, thus reducing the computational burden.

Dropout layers are interspersed at strategic intervals within the architecture to mitigate the risk of overfitting and potentially refining the network's learning capability [21]. One of the pivotal stages in this architecture is the data flattening process. After the Conv2D operations, the resultant feature maps are organized in a structured grid. Flattening transforms these grid-arranged kernels into a series of individual nodes, each holding specific numerical values. This sequential arrangement of nodes facilitates efficient processing in subsequent layers [22].

Following processing image data through our CNN, our attention turned to the numerical dataset. This subset was processed through several layers, each comprising four nodes, eventually resulting in an output of four nodes.

We employed the concatenate function to integrate the outputs from both the image and numerical data streams, effectively merging the two independent convolutional neural network pathways. Subsequent to this concatenation, the unified data was processed through one additional convolutional layer, eventually outputting to a singular output value.

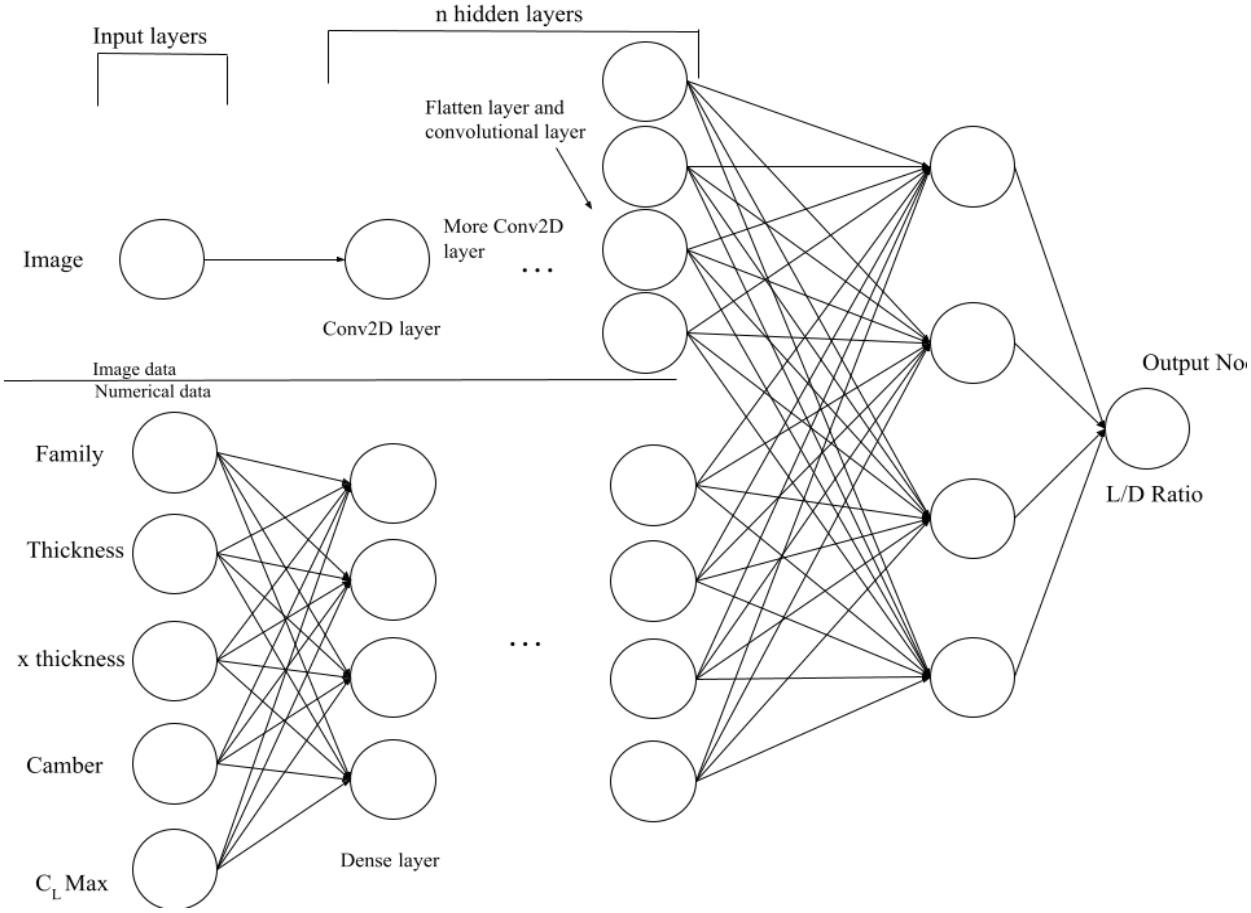

Figure 7: Basic architecture of the network. The top portion processes image data and the bottom processes numerical data. They are then combined.

The neural network was compiled using the root mean squared propagation optimizer better known as RMSProp with learning rate $1*10^{-4}$ and decay of $1*10^{-6}$ available in Keras. The RMSprop optimizer restricts the vertical oscillation of the model and thus the learning rate of the algorithm can be increased. We selected the mean squared error (MSE) as the loss function and

opted for the coefficient of determination, R^2, as the evaluation metric for accuracy. This choice provides insight into how well our predicted values match the actual data, with values closer to 1 indicating a better fit.

To ensure efficient computation and timely model training, we harnessed the computational capabilities of the T4 GPU, made available via Google Collaboratory. The Rectified Linear Unit (ReLU) function was chosen for all layers' activation functions.

4. Results and Discussion

After constructing our neural network architecture, a comprehensive series of hyperparameter tuning was conducted to hone the model's accuracy. The training phase involved feeding the model with our input dataset, allowing it to adjust its internal parameters to map the input to the desired output best.

For validation and to ascertain the efficacy of our model, we employed a testing dataset unseen during the training phase. This approach gives a more genuine assessment of the model's predictive capability, as it ensures that the model has not simply memorized the training data but has learned to generalize its predictions for new data.

We achieved noteworthy results in one of our most promising configurations, utilizing a model with three layers and training over 50 epochs with over 4 Conv2D layers, 3 numerical processing layers, and one combined layer. The model demonstrated the capability to predict the airfoil properties with commendable accuracy: approximately 58.6% of the predictions fell within a 10% margin of error relative to the true values.

Trial number	Amount of Epochs	Layers	Dropout	Accuracy rating (within 10% error)
1	30	1	.65	27%
2	50	1	.65	30.3%
3	30	3	.65	31.2%
4	50	3	.65	58.6%

Trial number	Amount of Epochs	Layers	Dropout	Accuracy rating (within 10% error)
1	30	1	.5	.6%
2	50	1	.5	31.5%
3	30	3	.5	52.8%
4	50	3	.5	6.4%

Trial number	Amount of Epochs	Layers	Dropout	Accuracy rating (within 10% error)
1	30	1	.4	28.7%
2	50	1	.4	0%
3	30	3	.4	0%
4	50	3	.4	36.2%

Utilizing a machine learning model to predict a specific value within a continuous spectrum, such as the L/D ratio for airfoils, inherently presents challenges on accuracy. This justifies our decision to classify a prediction as "reasonable" if it falls within a 10% error range. Such an approach provides a more practical measure of the model's efficacy, as demanding exact matches might be overly optimistic, especially in the early stages of such research.

The observed accuracy of approximately 58.6% within a 10% error margin, though promising, indicates that some aspects of our model or dataset might be refined for better results. One of the likely culprits we identified is the image data. The images, as processed, contained portions that extended beyond the actual graph of the airfoil. Such extraneous data can indeed introduce noise during the Conv2D layer processing, leading to less accurate predictions.

One potential improvement would be a more refined preprocessing of the image data. By cropping the images to encapsulate the airfoil graph tightly, we can eliminate unnecessary data and focus the model on the most pertinent information. Such an adjustment might allow the Conv2D layers to derive features more representative of the actual airfoil shape, potentially leading to more accurate predictions.

5. Conclusions

In this research, a machine learning model took in image data of an airfoil alongside geometric properties and predicted the corresponding lift-drag ratio properties of the wing, which is directly correlated to the efficiency and fuel usage needed to fly. The dataset consisted of thousands of airfoils from over 30 different airfoil manufacturers. Training over 12 different networks, differing levels of accuracy were observed in each individual model. Some models performed noticeably better than other networks. The best network, which was trained with over three layers and 50 epochs with a dropout of .4, predicted over 58.6% of the airfoils within a 10% error of the actual value, a respectable value considering the basic and free equipment used in processing. This compares to the millions of dollars used to maintain and build wind tunnels.

With models that predict over half of the airfoil’s lift/drag properties accurately, this displays the potential and the ability for machine learning models to predict with greater accuracy. While 58.6% accuracy is decent, it can certainly be improved. With more hyperparameter tuning and more epochs of training, it is likely that the accuracy of the model

can be brought up to 90% and above. In addition, with better image quality, the limit of our general accuracy can certainly be raised.

The current dataset consists of data where Reynold's Number is 3 million. To more accurately simulate small amateur planes and large passenger/cargo planes, Maximum lift coefficient and maximum lift/drag ratio data Reynold's Numbers of 1 million and 12 million can be used as input and output, respectively to train machine learning models that are more equipped to assist fuel efficiency on commonly used airplanes. In addition, more data from the bigfoil website such as compressibility effects and even incorporation coefficient of moment data could make more accurate predictions. Finally, providing more detailed pictures as well as having a stronger GPU to process these pictures would allow hyperparameter tuning to occur quicker and the convolutional neural network to produce more accurate results.

Besides just making accurate predictions to the aerodynamics of an airfoil, a machine learning model with large amounts of training data may also be able to reveal attributes that make successful airfoils and help make significant improvements to the aerodynamic properties of an airplane, significantly decreasing carbon dioxide exhaust.

The future of aerodynamics, fueled by machine learning, seems promising. Machine learning algorithms can certainly match the accuracy and precision of computer simulations and wind tunnel testing without the major costs. But more importantly, models like ours assist in designing more fuel-efficient wings, but they can also potentially reduce aviation's carbon footprint.

Acknowledgments

I want to thank Dr. Jeremy Keys, a student at Northwestern University, who introduced the many essential aerospace concepts including airfoil physics and airfoil design. This dataset was also introduced to me by him.

References

[1] Milne-Thomson, Louis Melville. Theoretical aerodynamics. Courier Corporation, 1973.

[2] Keys, J. "So you want to be….". Robert R. McCormick School of Engineering and Applied Science at Northwestern. 2023.

[3] Sadraey, Mohammad, and Dr Müller. "Drag force and drag coefficient." M. Sadraey, Aircraft Performance Analysis. VDM Verlag Dr. Müller (2009).

[4] Wegener, Peter P. What Makes Airplanes Fly?: History, Science, and Applications of Aerodynamics. Springer, 1998.

[5]Lissaman, P. B. S. "Low-Reynolds-number airfoils." Annual review of fluid mechanics 15.1 (1983): 223-239.

[6]Benson, Tom. "Geometry Definitions." NASA, www.grc.nasa.gov/www/k-12/VirtualAero/BottleRocket/airplane/geom.html. Accessed 05 Oct. 2023.

[7] Benson, Tom. “Inclination Effects on Lift.” *NASA*, www.grc.nasa.gov/www/k-12/VirtualAero/BottleRocket/airplane/incline.html. Accessed 05 Oct. 2023

[8] Leishman, J. Gordon. “Mach Number & Reynolds Number.” *Introduction to Aerospace Flight Vehicles*, Embry-Riddle Aeronautical University, 2022, eaglepubs.erau.edu/introductiontoaerospaceflightvehicles/chapter/mach-number-and-reynolds-number/#:~:text=The%20Mach%20number%20is%20defined,inertial%20forces%20to%20viscous%20forces. Accessed 05 Oct. 2023.

[9] Van Dam, C. P. "The aerodynamic design of multi-element high-lift systems for transport airplanes." Progress in Aerospace Sciences 38.2 (2002): 101-144.

[10] Drela, Mark. "Pros & cons of airfoil optimization." Frontiers of Computational Fluid Dynamics 1998. 1998. 363-381.

[11] Aitcheson, Pete. “NASA Wind Tunnels Final Report 20150813.” NASA, 13 Aug. 2015, www.hq.nasa.gov/office/codej/codejx/Assets/Docs/2015/NASA_Wind_Tunnels_Final_Report_20150813-TAGGED.pdf.

[12] Song, Xueyi, et al. "Airfoil optimization using a machine learning-based optimization algorithm." Journal of Physics: Conference Series, vol 2217, no 1,2021,pp. 1-9, https://doi.org/10.1088/1742-6596/2217/1/012009.

[13] S. Bhantnagar, Y. Afshar, S. Pan, K. Duraisamy, and S. Kaushik, “Prediction of aerodynamic flow fields using convolutional neural networks,”

Computational Mechanics, vol. 64, no. 2, pp. 525–545, 2019.

[14] V. Sekar, Q. Jiang, C. Shu, and B. C. Khoo, “Fast flow field prediction over airfoils using deep learning approach,” Physics of Fluids, vol. 31, no. 5, p. 057103, 2019.

[15] X. Hui, J. Bai, H. Wang, and Y. Zhang, “Fast pressure distribution prediction of airfoils using deep learning,” Aerospace Science and Technology, vol. 105, p. 105949, 2020.

[16] X. Guo, W. Li, and F. Iorio, “Convolutional neural networks for steady flow approximation,” in Proceedings of the 22nd ACM SIGKDD international conference on knowledge discovery and data mining, 2016, pp. 481–490.

[17] Y. Zhang, W. J. Sung, and D. N. Mavris, “Application of convolutional neural network to predict airfoil lift coefficient,” in AIAA/ASCE/AHS/ASC Structures, Structural Dynamics, and Materials Conference, 2018, p. 1903.

[18] Moin, Hassan, et al. "Airfoil’s Aerodynamic Coefficients Prediction using Artificial Neural Network." 2022 19th International Bhurban Conference on Applied Sciences and Technology (IBCAST). IEEE, 2022.

[19] Takaki, Ryoji. "Aerodynamic characteristics of NACA4402 in low Reynolds number flows." Japan Society of Aeronautical Space Sciences 54.631 (2006): 367-373.

[20] Li, Zewen, et al. "A survey of convolutional neural networks: analysis, applications, and prospects." IEEE transactions on neural networks and learning systems (2021).

[21] Santos, Claudio Filipi Gonçalves Dos, and João Paulo Papa. "Avoiding overfitting: A survey on regularization methods for convolutional neural networks." ACM Computing Surveys (CSUR) 54.10s (2022): 1-25.

[22] Tan, M., Mike Xu and David Moss. 2021 "Tera-OPs Photonic Convolutional Neural NetworksBased on Kerr Microcombs" Preprints. https://doi.org/10.20944/preprints202102.0549.v1